Supporting Information

Hetero-symbiotic $Na_{3.12}Fe_{2.44}(P_2O_7)_2$-$Na_4Fe_3(PO_4)_2(P_2O_7)$/reduced graphene oxide for superior electrochemical sodium storage

Xiaozhong Zhou,*[a] Jiangwei Deng,[a] Zhengfeng Zhang,[b] Sihang Liu,[a] Yan Zhang,[a] Xiaoyan Zheng,[a] Dengfei Sun [a] and Yaoxia Yang [a]

[a] Key Laboratory of Eco-functional Polymer Materials of the Ministry of Education, College of Chemistry and Chemical Engineering, Northwest Normal University, Lanzhou 730070, Gansu, China

[b] State Key Laboratory of Solid Lubrication, Lanzhou Institute of Chemical Physics, Chinese Academy of Sciences, Lanzhou 730000, China.

*Corresponding author, E-mail: zxz20004@163.com (X. Zhou), ORCID: 0000-0001-5366-0545

Calculation procedure for the carbon content in samples

During the TGA testing at air atmosphere, the oxidization and further combustion of carbonaceous components causes the mass loss, whereas the oxidizations of both Fe^{2+} to Fe^{3+} and $P_2O_7^{4-}$ to PO_4^{3-} result in weight increment. If one equivalent of Fe^{2+} is oxidized to Fe^{3+}, half an equivalent of oxygen is needed. And one equivalent of oxygen is added for the oxidization of $P_2O_7^{4-}$ to form PO_4^{3-}. Based on the chemical formula, upon complete oxidation per mole of NFPO (or NFPP), the uptakes of 3.22 (or 2.5) moles of oxygen atoms is necessary, corresponding to a weight gain of 9.26% (or 6.41%). According to the whole pattern fitting (WPF) Rietveld refinement results of XRD patterns, the relative NFPO contents in NFPO-NFPP (71.3%) and NFPO-NFPP/rGO (67.8%) composites were estimated. So that, complete oxidation of Fe^{2+} and $P_2O_7^{4-}$ in the samples results in relative weight gain rates (marked as *a*) of 7.23% and 7.33% for the NFPO-NFPP and NFPO-NFPP/rGO, respectively. As shown in Fig. 1i in this revised manuscript, the actual weight gain rates (marked as *b*) of the two samples are 1.05 wt% (NFPO-NFPP) and -2.89 wt% (NFPP-NFPO/rGO) when the temperature arises 620 °C. Thus, the carbon contents (marked as *x*) in composites can be estimated with the following equation (Eq. 1) to be 5.76 wt% (NFPO-NFPP) and 9.72 wt% (NFPO-NFPP/rGO), respectively. Assuming that the $C_2O_4^{2}$-derived carbon content remains constant, the rGO content can be estimated to be 3.96 wt%.

$$(1-x)\cdot a-x=b \qquad \text{Eq. (1)}$$

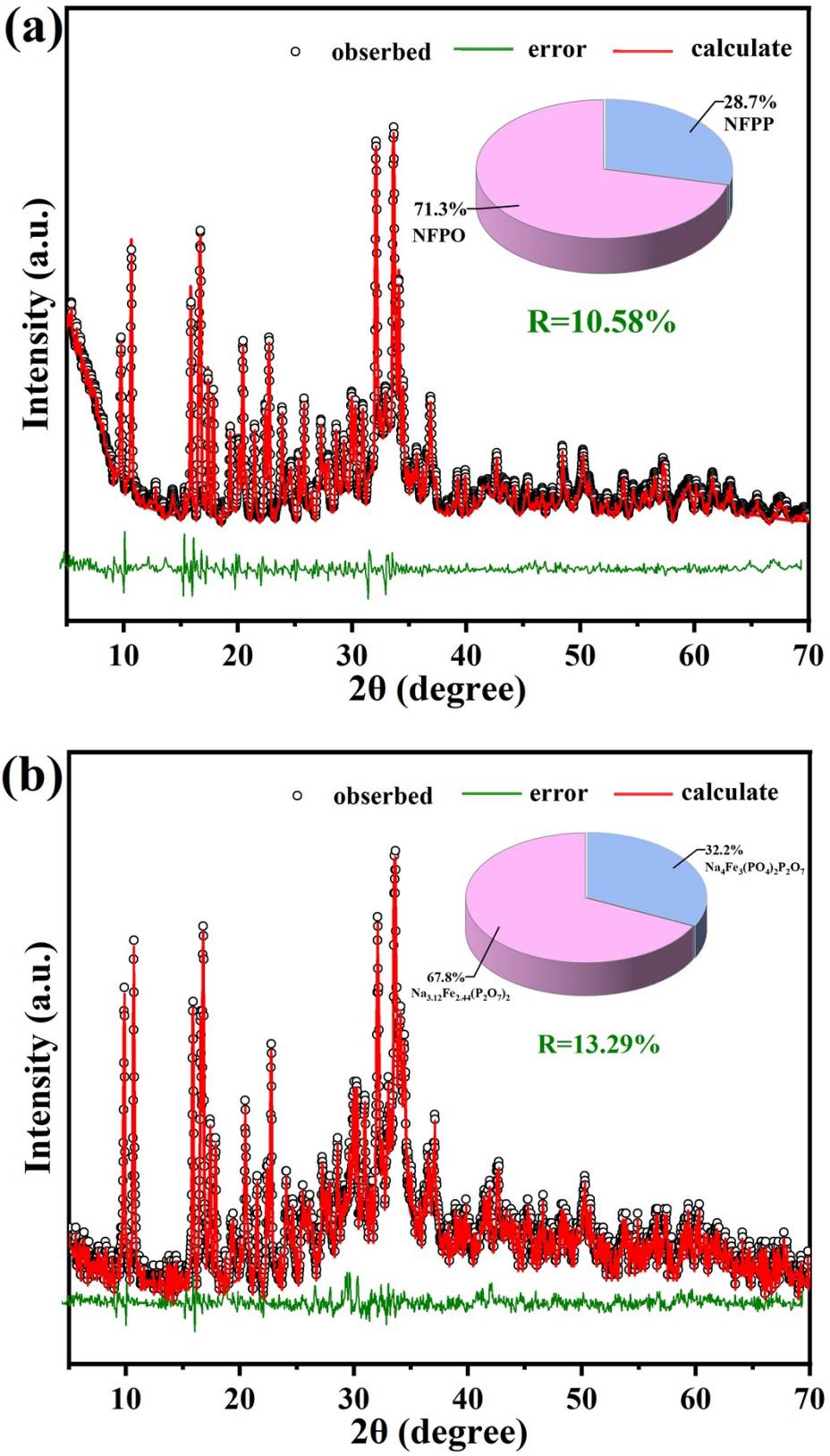

Fig. S1. Rietveld refined XRD patterns of (a) NFPO-NFPP and (b) NFPO-NFPP/rGO samples.

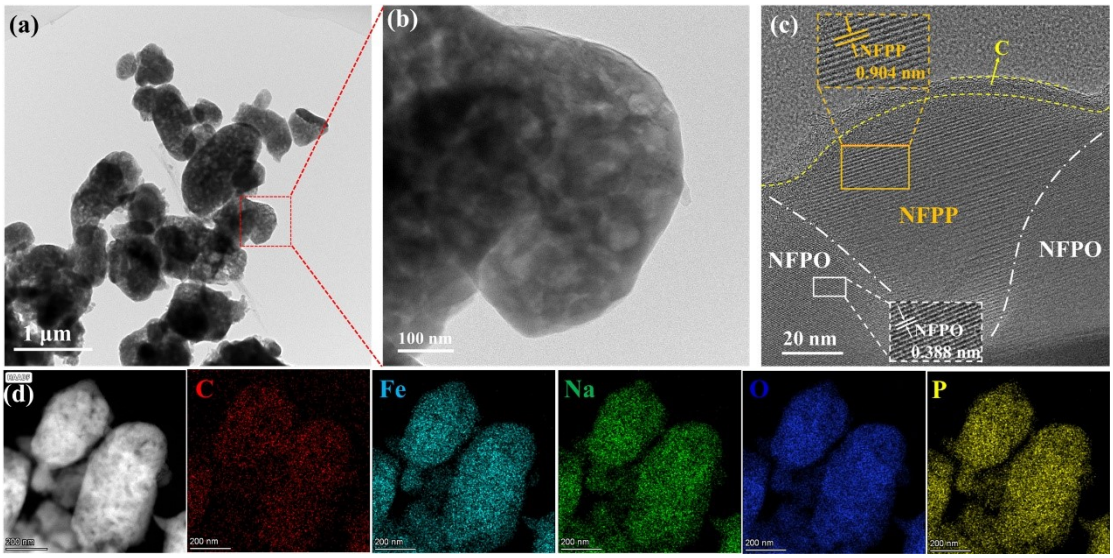

Fig. S2. (a,b) TEM, (c) HRTEM, and (d) STEM-HADDF with their corresponding EDS mapping images of NFPO-NFPP sample.

Table S1. Comparison on electrochemical properties between NFPO-NFPP/rGO and previously-reported NFPO-based cathodes

Samples	Reversible capacity (mAh g^{-1})	Rate capability (mAh g^{-1})	Capacity retention rate	Ref.
NFPO-NFPP/rGO	107.2 at 0.5 C	95.1 at 10 C, 93.3 at 20 C	86.8% after 500 cycles at 1 C 80.3% after 1000 cycles at 10 C	**This paper**
3D-porous $Na_{3.12}Fe_{2.44}(P_2O_7)_2$	108.13 at 0.1 C	95.94 at 1 C	95.1% after 400 cycles at 5 C	[1]
Hollow $Na_{3.12}Fe_{2.44}(P_2O_7)_2$	104 at 0.5 C	79 at 5 C	93.1% after 500 cycles at 10 C	[2]
$Na_{3.12}Fe_{2.44}(P_2O_7)_2$/rGO	109 at 0.1 C	78 at 10 C	70% after 500 cycles at 10 C	[3]
$Na_{3.12}Fe_{2.44}(P_2O_7)_2$/r-GO	116.9 at 0.1 C	77.2 at 10 C	88.82% after 5000 cycles at 20 C	[4]
$Na_{3.12}Fe_{2.44}(P_2O_7)_2$/C	118.2 at 0.1 C	57.5 at 20 C, 45.7 at 30 C	97.5% after 800 cycles at 1 C	[5]
$Na_{3.12}Fe_{2.44}(P_2O_7)_2$/C	101.6 at 1 C	32.9 at 10 C	79% after 3700 cycles at 2 C	[6]
$Na_{3.12}Fe_{2.44}(P_2O_7)_2$/C	97 at 1 C	80 at 6 C	94.4% after 600 cycles at 20 C	[7]
$Na_{3.12}Fe_{2.44}(P_2O_7)_2$/C	107 at 0.05 C	88 at 2 C	95% after 200 cycles at 5 C	[8]
$Na_{3.12}Fe_{2.44}(P_2O_7)_2$/MWCNT	>100 at 0.15C	40.1 at 1.5 C	--	[9]
x$NaFePO_4$-$Na_{3.12}Fe_{2.44}(P_2O_7)_2$	125.2 at 0.1 C	93.3 at 60 C	87% after 3000 cycles at 20 C	[10]
$NaTiP_2O_7$ coated $Na_{3.12}Fe_{2.44}(P_2O_7)_2$	108.4 at 0.1 C	84.7 at 20 C, 66.2 at 100 C	92.66% after 3000 cycles at 10 C	[11]
AlF_3-coated $Na_{3.12}Fe_{2.44}(P_2O_7)_2$	130 at 0.1 C (60 °C)	61.5 at 20 C, 52.5 at 50 C	70% after 6000 cycles at 50 C	[12]
$Na_{3.08}Fe_{2.44}(P_2O_{6.98})_2F_{0.04}$	116.4 at 0.05 C	78.4 at 20 C 61.6 at 80 C	86.3% after 20000 cycles at 50 C	[13]
Si^{4+}-doped $Na_{3.12}Fe_{2.44}(P_2O_7)_2$	116.6 at 0.05 C	67.2 at 50 C	84.8% after 14000 cycles at 20 C	[14]
Ni/Mn-doped $Na_{3.12}Fe_{2.44}(P_2O_7)_2$	114 at 20 mA g^{-1}	97 at 1 A g^{-1}	80.04% after 1000 cycles at 1 A g^{-1}	[15]
Ti^{3+}-doped $Na_{3.12}Fe_{2.44}(P_2O_7)_2$	109.8 at 23.4 mA g^{-1} (0.2 C)	48.3 at 5.85 A g^{-1} (50 C)	90.3% after 4000 cycles at 5 C	[16]
Mg^{2+}-doped $Na_{3.12}Fe_{2.44}(P_2O_7)_2$	110.5 at 0.1 C	77.2 at 10 C, 68.6 at 50 C	79.1% after 3000 cycles at 20 C	[17]

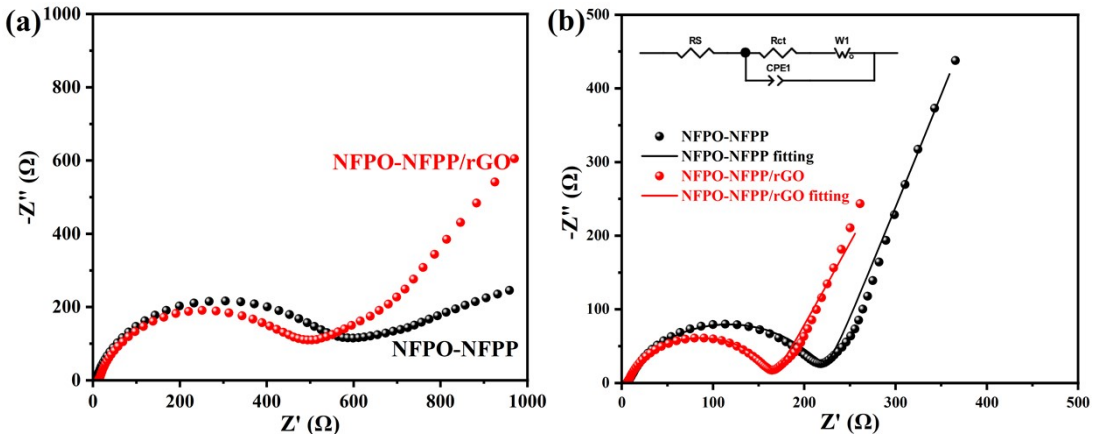

Fig. S3. EIS plots and equivalent circuit fitting results of NFPO-NFPP and NFPO-NFPP/rGO electrodes (a) before and (b) after 20 cycles at 0.5 C and the equivalent circuit model insert in (b).

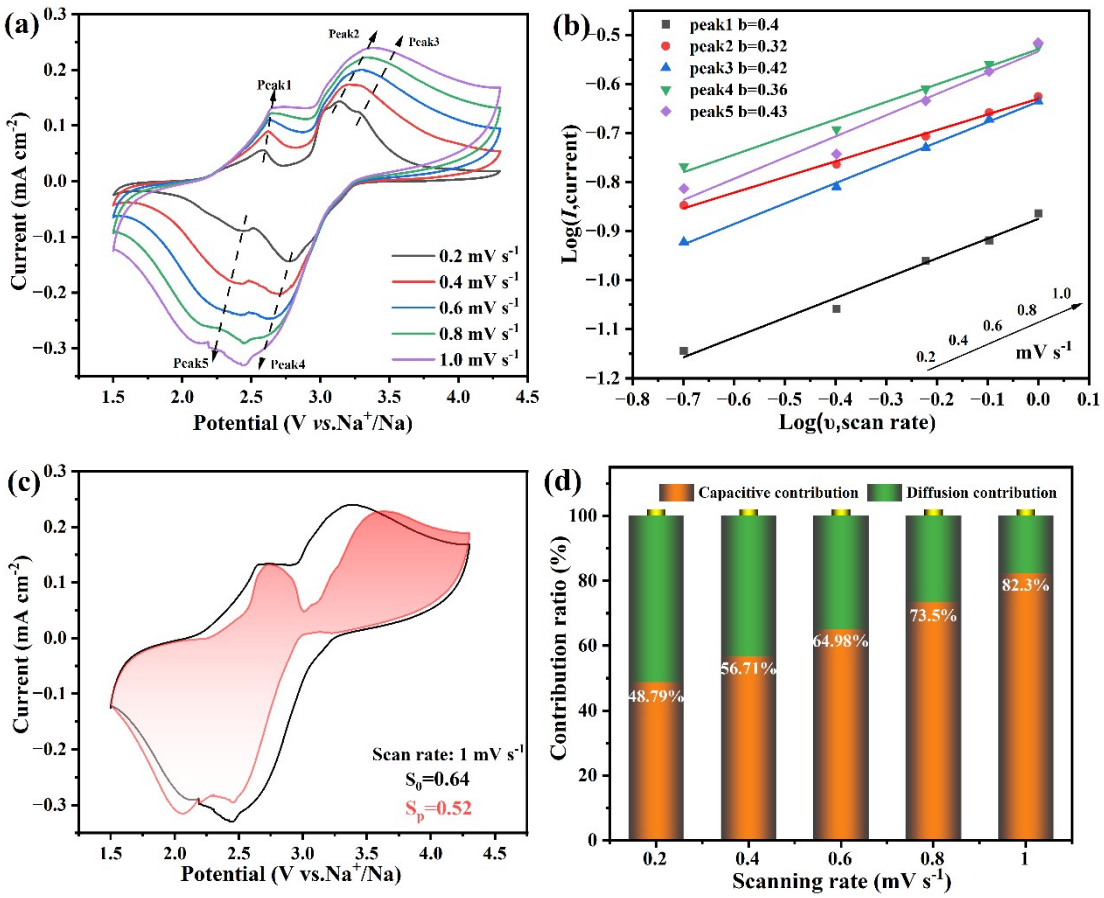

Fig. S4. Electrochemical kinetics of NFPP-NFPO for sodium storage. (a) CV curves at sweep rates varied from 0.2 to 1.0 mV s^{-1}, (b) log(*i*)-log(*v*) linear relationship plots, (c) capacitive contributions at 1 mV s^{-1}, (d) capacitive and diffusion-controlled contribution ratios at different scan rates.

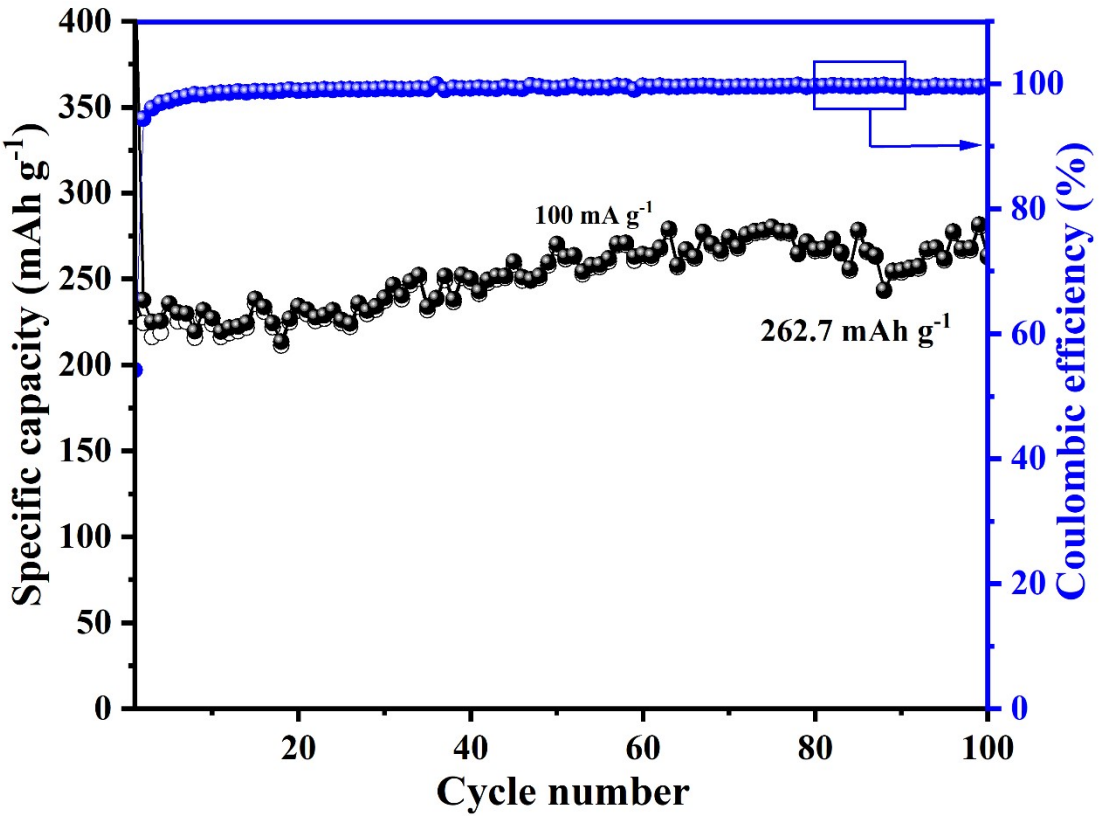

Fig. S5. Cycling performance of HC anode at 100 mA g^{-1}

Reference

1. Y. Xu, J. Lu, X. Chen, Y. Li, K. Zhang, S. Zhang, Y. Yao and J. Hu, J. Alloy. Compd., 2025, 1044, 184622.
2. B. Lin, Q. Li, B. Liu, S. Zhang and C. Deng, Nanoscale, 2016, 8, 8178-8188.
3. H. J. Song, K.-H. Kim, J.-C. Kim, S.-H. Hong and D.-W. Kim, Chem. Commun., 2017, 53, 9316-9319.
4. B. Liu, Y. Zou, S. Chen, H. Zhang, J. Sun, X. She and D. Yang, Chem. Eng. J., 2019, 365, 325-333.
5. Z. Yang, P. Wang, C. Xing, J. Chen, P. Yang, J. Zhou, L. Chen, S. Tao, Z. Zhang, C. Wu and L. Fei, ACS Nano, 2025, 19, 40404-40415.
6. Z. Cao, X. Hu, Y. Wang, Y. Xu, Y. Zhou, X. Cao and S. Liang, J. Mater. Chem. A, 2024, 12, 28130-28138.
7. C. Deng, S. Zhang, H. Wang and G. Zhang, Nano Energy, 2018, 49, 419-433.
8. B. Lin, S. Zhang and C. Deng, J. Mater. Chem. A, 2016, 4, 2550-2559.
9. Y. Niu, M. Xu, C. Cheng, S. Bao, J. Hou, S. Liu, F. Yi, H. He and C. M. Li, J. Mater. Chem. A, 2015, 3, 17224-17229.
10. Z. Liu, Y. Cao, N. Wang, H. Yang, H. Zhang, X. Xu, N. Wang, J. Xu, Y. Liu, J. Zhang and Y. Xia, Nano Res., 2024, 17, 8119-8125.
11. H. Zhang, Q. Li, X. Xu, H. Yang, G. Li, Z. Liu, M. Liao, J. Xu, X.-L. Li, N. Wang, J. Zhang, H. Peng and Y. Cao, J. Colloid Interface Sci., 2025, 678, 20-29.
12. Y. Zhang, J. Zhang, X. Li, G. Chen, B. Zhang, H. Liu, Y. Wang and Z.-F. Ma, Chem. Eng. J., 2022, 430, 132708.
13. X. Wang, J. Li, Q. Wang, H. Li, J. Liang, L. Zhang, X. Wang, K. Ding, H. Liu, Z. F. Ma and Y. Wang, Adv. Energy Mater., 2025, 15, 2502300.
14. X. Wang, L. Zhang, Q. Wang, J. Li, X. Wang, L. He, J. Xu, K. Ding, H. Liu, Z. F. Ma and Y. Wang, Adv. Funct. Mater., 2026, 36, e29331.
15. R. Zhou, X. Wen, Z. Tang, C. Wang, T. Wang, L. Wang, H. Zhong and Y. Jiang, ACS Appl. Energy Mater., 2024, 7, 1756-1765.
16. L. Zhu, S. Xiang, M. Wang, D. Sun, X. Zhang, L. Fu, X. Huang, Y. Tang, Q. Zhang and H. Wang, Adv. Funct. Mater., 2025, 35, 2419611.
17. Y. Zhang, J. Zhang, T. Shao, X. Li, G. Chen, H. Liu and Z.-F. Ma, ACS Appl. Mater. Interfaces, 2022, 14, 14253-14263.